Protective effects of tiger milk mushroom extract (xLr®) against UVB irradiation in *Caenorhabditis elegans via* DAF-16 anti-oxidant regulation

Panthakarn Rangsinth [a,b], Rajasekharan Sharika [a,b], Chanin Sillapachaiyaporn [c], Sunita Nilkhet [c], Kamonwan Chaikhong [c], Kanika Verma [c], Anchalee Prasansuklab [d], Szu-Ting Ng [e], Chon-Seng Tan [e], Shin-Yee Fung [f], Tewin Tencomnao [c], Siriporn Chuchawankul [a,b,*]

[a] *Immunomodulation of Natural Products Research Unit, Faculty of Allied Health Sciences, Chulalongkorn University, Bangkok 10330, Thailand*
[b] *Department of Transfusion Medicine and Clinical Microbiology, Faculty of Allied Health Sciences, Chulalongkorn University, Bangkok 10330, Thailand*
[c] *Department of Clinical Chemistry, Faculty of Allied Health Sciences, Chulalongkorn University, Bangkok 10330, Thailand*
[d] *College of Public Health Sciences, Chulalongkorn University, Bangkok 10330, Thailand*
[e] *LiGNO Biotech Sdn Bhd., Jalan Perindustrian Balakong Jaya 2/2, Taman Perindustrian Balakong Jaya 2, 43300 Balakong jaya, Selangor, Malaysia*
[f] *Medicinal Mushroom Research Group (MMRG), Department of Molecular Medicine, Faculty of Medicine, Universiti Malaya, 50603 Kuala Lumpur, Malaysia*

ABSTRACT

Background and aim: A critical causative factor of oxidative stress and inflammation leading to several skin complications is ultraviolet-B (UVB) irradiation. *Lignosus rhinocerus* (LR), or tiger milk mushroom, is native to Southeast Asia. Cold water extract of an LR cultivar, TM02® (xLr®) is a promising anti-oxidant and anti-inflammatory source. However, the effects of xLr® on UVB-induced photoaging have never been elucidated.
Experimental procedure: This study investigated the protective effects of xLr® and its high, medium, and low molecular weight (HLR, MLR, and LLR, respectively) fractions against UVB irradiation using *in vivo Caenorhabditis elegans* (*C. elegans*) model.
Results and conclusion: The investigation revealed a significant lifespan extension of xLr® and its fractions in UVB-irradiated *C. elegans*, which could be mediated by the regulation of genes associated with anti-oxidant (*daf-16* and *sod-3*) and apoptosis (*cep-1*, *hus-1*, *ced-13*, and *egl-1*) pathways. xLr® significantly reduced the ROS production in *C. elegans* and increased the DAF-16 nuclear translocation compared to untreated worms. Additionally, the SOD-3 expression was increased in the xLr®-treated worms. Hence, it suggests that the different components in xLr® work synergistically to protect against UVB irradiation. Our findings may be beneficial for the application of xLr® as a treatment against UVB-induced cellular damage and photoaging.

1. Introduction

Skin aging is a spontaneous process that occurs while growing older over time. Many factors contribute to skin aging including intrinsic and extrinsic factors. Intrinsic factors refer to genetics, hormones, and metabolisms, while extrinsic factors refer to lifestyle and environmental factors such as sunlight exposure.[1] Sunlight is composed of three different ultraviolet (UV) radiations, including UVA, UVB, and UVC.

Accumulating evidence demonstrates that UVB prominently plays a significant role in promoting aging in comparison to UVA and UVC.[1–3] UVB directly damages the DNA by enhancing the production of reactive oxygen species (ROS) and inducing oxidative stress, resulting in altered gene expression that consequently causes senescence, cell cycle arrest, and cell death. Moreover, when skin is exposed to UVB, it triggers a cascade of immune responses, including inflammations. Excessive UVB-induced inflammation can contribute to skin aging and increased risk of skin cancer.[4] Therefore, the inhibition of oxidative stress and

List of abbreviations

ABTS	2,2-Azino-bis(3-ethylbenzothiazoline-6-sulfonic acid)
DCFH-DA	diacetyldichlorofluorescein diacetate
DMSO	Dimethyl sulfoxide
GFP	green fluorescence protein
HLR	high molecular weight fraction of cold water extract of *Lignosus rhinocerus* (xLr®)
LC-MS	Liquid chromatography mass spectrometry
LLR	low molecular weight fraction of cold water extract of *Lignosus rhinocerus* (xLr®)
LR	*Lignosus rhinocerus*
MLR	medium molecular weight fraction of cold water extract of *Lignosus rhinocerus* (xLr®)
MTT	(3-(4,5-dimethylthiazol-2-yl)-2,5-diphenyltetrazolium dromide
NGM	nematode growth medium
qRT-PCR	quantitative Reverse Transcriptase-Polymerase Chain Reaction
ROS	Reactive oxygen species
xLr®	Cold water extract of *Lignosus rhinocerus* cultivar TM02®

inflammation could attenuate the adverse effects of UVB exposure. Currently, there is much evidence that herbal natural products are rich source of bioactive compounds including vitamin, phenolic, flavonoid, and glucan, contributing to their therapeutic potential in managing conditions associated with inflammation and oxidative stress.[5–8] Therefore, utilizing these beneficial properties from natural products may establish protective effects against UVB-induced toxicity.

Lignosus rhinocerus (Cooke) Ryvarden, also commonly known as tiger milk mushroom, belongs to the Polyporaceae family and is considered a valuable traditional medicine. The mushroom is found in South China, Thailand, Malaysia, Indonesia, Philippines, Papua New Guinea, New Zealand, and Australia.[9] It has been illustrated that tiger milk mushroom extracts have anti-oxidant,[10–14] anti-inflammation,[15] anti-cancer,[16–20] anti-bacterial,[21] and anti-viral[22–24] properties. Recently, its cold water extract (xLr®) was reported to enhance stress resistance and capable of extending the lifespan of *Caenorhabditis elegans* (*C. elegans*).[25] Furthermore, xLr® and its high (HLR), medium (MLR), and low (LLR) molecular weight fractions were found to possess anti-inflammatory activity *via* inhibition of lipopolysaccharide-induced TNF-α production as revealed in RAW 264.7 macrophage cells and anti-acute inflammation of carrageenan-induced paw edema in rats.[26] However, the effects of xLr® and its fractions on UVB-induced photoaging have not been elucidated.

In this study, the effects of xLr® and its fractions against UVB-induced toxicity were investigated *in vivo* using nematode *C. elegans*. The findings may be beneficial for the application of xLr® as a treatment against UVB-induced toxicity.

2. Materials and methods

2.1. Preparation of xLr® and its fractions

The sclerotia of *L. rhinocerus* cultivar TM02® was provided by LiGNO Biotech Sdn. Bhd. (Selangor, Malaysia). The internal transcribed spacer (ITS) regions of the ribosomal DNA of the mushroom were identified.[27] Cold water extract of *L. rhinocerus* TM02® (xLr®) and its fractions, high (HLR), medium (MLR), and low (LLR) molecular weight were prepared as previously described.[26] Briefly, the freeze-dried sclerotial powder was stirred in distilled water at 4 °C for 24 h xLr® was fractionated using Sephadex G-50 (Sigma-Aldrich, USA) Superfine column (v = 112 mL) and eluted with 0.05 M ammonium acetate buffer at 0.5 mL/min. HLR

fraction appeared at void volume (mol. wt. >10 kDa dextran or 30 kDa protein) while LLR fraction appeared at bed volume. MLR fraction appeared between void and bed volume.

2.2. Measurement of glucan, phenolic and flavonoid content

The total glucan, β-glucan, and α-glucan contents of xLr® and its fractions were quantified using the protocol adapted from the Megazyme™ β-Glucan Assay Kit (Yeast and Mushroom) per the manufacturer's instructions (Megazyme© Ltd., Bray, Wicklow County, Ireland). The d-glucose (100 μg) was used as the standard for the method calculation. After the reaction was completed, samples (200 μL) were transferred into a 96-well plate, and the absorbance was read at 510 nm using a microplate reader EnSpire® Multimode Plate Reader (PerkinElmer, Waltham, MA, USA). Mega-Calc™ Data Calculator was utilized to determine the total glucan, α-glucan, and β-glucan contents calculated from sample weight and volume. The total phenolic content was determined by the Folin-Ciocalteu method, while the total flavonoid content was determined by the aluminium chloride ($AlCl_3$) colorimetric method. The assays were performed using a microplate format as previously described.[28] The absorbance was measured. The total phenolic content was calculated from a standard calibration curve of gallic acid, and the results were expressed as mg of gallic acid equivalent (GAE) per g of dry weight extract. The content of total flavonoids was calculated from a standard calibration curve of quercetin. The results were expressed as mg of quercetin equivalent (QE) per g of dry-weight extract.

2.3. Free radical scavenging assay

The 2,2′-azinobis-(3-ethylbenzothiazoline-6-sulfonic acid) (ABTS) assay was used to evaluate the free radical scavenging activity of the extract based on its hydrogen atom- or electron-donating capacity to neutralize the stable free radical cation ABTS (ABTS•+), accompanied by a color change from green to colorless. The assay was performed following the previous report.[28] The absorbance was measured at 734 nm using a microplate reader EnSpire® Multimode Plate Reader (PerkinElmer, Waltham, MA, USA). Radical scavenging activity was expressed as the percent inhibition of the ABTS•+ radicals calculated by the following equation: % Inhibition = 100 × [Absorbance (Abs) of control - (Abs of sample - Abs of blank)/Abs of control]. Ascorbic acid (vitamin C) was used as a positive control.

2.4. C. elegans culture and treatment conditions

The *C. elegans* strain used in this study was wild type N2 Bristol, transgenic strains CF1553 [muls 84[(pAD76) sod-3pGFP + rol-6 (su1006)], and TJ356 [daf-16daf-16a/bGFP + rol-6]. The worms were cultured with nematode growth medium (NGM) containing *E. coli* OP50 as a food source and kept in an incubator at 20 °C. The nematodes and *E. coli* OP50 were obtained from Caenorhabditis Genetics Center (CGC), University of Minnesota, USA.

Age synchronization of the worms was achieved by isolating eggs from gravid hermaphrodites, by adding lysis solution containing 5 M NaOH and 5 % NaOCl, followed by vortex mixing for 10 min and centrifuging for 2 min at 2000 rpm. Then, the supernatant was removed, and the pellet was washed twice with M9 buffer. Further, the pellet containing eggs was resuspended in M9 buffer and kept at 20 °C for hatching overnight.

For subsequent experiments, the worms were treated with xLr®, and its fractions. The treatments were prepared in S-medium containing *E. coli* OP50 (OD_{600} = 1.0) and lawn on NGM agar plates.

2.5. Survival assay under oxidative stress induced by juglone

Age-synchronized L1 larvae stage worms were divided into groups of

50 and treated with different concentrations of the extracts diluted in S-medium containing *E. coli* OP50. After 48 h of treatment at 20 °C, the pro-oxidant juglone (a naphthoquinone from *Juglans regia*) was added to a final concentration of 80 μM, which is a lethal concentration before incubation at 20 °C for an additional 24 h. Afterward, the number of worms which are dead and alive were counted.

2.6. Lifespan assay in UVB-irradiated C. elegans

C. elegans was irradiated with UVB at a dose of 100 J/m^2 or 100×10^3 mJ/m^2 (Philips Ultraviolet-B TL 20W/01 RS lamp), which is a suitable dose that causes damage to *C. elegans* cells and shorten the worm's lifespan.[29] Irradiation doses were calculated using the following formula: dose (mJ/cm^2) = exposure time (s) × intensity (mW/cm^2). In each UVB exposure experiment, the UVB intensity was priorly measured to ensure accurate dosing. The L4 larval stage was placed on NGM agar plates supplemented with the extracts in the *E. coli* OP50 lawn as a food source and cultured at 20 °C for 24 h. When irradiating *C. elegans*, the covers of the NGM plates were removed, and no liquid was to be on the culture medium's surface to exclude the liquid medium's interference with the radiation dosage.

2.7. Pharyngeal pumping assay

To determine the age-related decline in muscle function by pharyngeal pumping rate, the synchronized L4 worms were lawn on NGM agar containing *E. coli* OP50 with treatments. The adult worms were transferred to the new NGM plate every day during the reproductive period. The pumping activities were measured on day 4, 8, 12, and 16 of adulthood. For each worm, the pumping frequency was recorded for 1 min.

2.8. Induction of SOD-3 in GFP-tagged strain

The transgenic *C. elegans* strain CF1553 was used for the study. To induce oxidative stress, the worms were irradiated with UVB at a dose of 100 mJ/cm^2, and the treatments were performed as in the lifespan assay mentioned above. The irradiated worms were transferred into *E. coli* OP50 lawn as a food source and cultured at 20 °C for 24 h. After 24 h, the worms were paralyzed using 10 mM sodium azide[30] on a glass slide and fluorescence imaging was taken using a confocal microscope (Leica Stellaris 5) at 20× magnification. The expression of SOD-3 at the pharynx region was used to analyze the fluorescence intensity using Image J software (National Institute of Health, Bethesda, MD, USA).

2.9. Assessment of intracellular DAF-16 translocation

TJ356 *C. elegans* containing GFP reporter of DAF-16 was used for the study. The experiments were performed as in the assay mentioned above. The irradiated worms were transferred into *E. coli* OP50 lawn as a food source and cultured at 20 °C for 24 h. After 24 h, the worms were paralyzed using 10 mM sodium azide[30] on a glass slide and fluorescence imaging was taken using a confocal microscope (Leica Stellaris 5) at 10× magnification. Fluorescence intensity was taken using Image J software (National Institute of Health, Bethesda, MD, USA).

2.10. Intracellular ROS activity

The intracellular ROS induced by UVB exposure was assessed by using DCFH-DA (a fluorogenic probe). Wild-type *C. elegans* were irradiated with UVB, and the treatments were performed as in the assay mentioned above. The irradiated worms were transferred into *E. coli* OP50 lawn as a food source and cultured at 20 °C for 24 h. After that, the worms were exposed to DCFH-DA for 30 min at dark conditions and washed thoroughly before paralyzing using a 10 mM sodium azide[30] on a glass slide and fluorescence imaging was taken using a confocal

microscope (Leica Stellaris 5) at 10× magnification. Fluorescence intensity was measured using Image J software (National Institute of Health, Bethesda, MD, USA).

2.11. Real-time qRT-PCR

Total RNA from *C. elegans* was extracted using Trizol reagent following the manufacturer's instructions. The amount of RNA was measured by absorbance at 260 nm. One microgram of total RNA was used for cDNA synthesis using AccuPower RT PreMix (Bioneer Co., South Korea) and Oligo(dT) 17 primer. Real-time PCR analysis was used to determine the mRNA expression level. The reaction was performed in the Exicycler™ version 3.0 (Bioneer Co.). The amplification was done using Greenstar™ qPCR Premix (Bioneer Co.). The sequence of primers was detailed as *daf-16*: 5′- TTTCCGTCCCCGAACTCAA -3′ and 5′-ATTCGCCAACCCATGATGG -3′, *sod-3*: 5′- TTCGAAAGGGAATCTAAAAGAAG -3′ and 5′- GCCAAGTTGGTCCAGAAGATAG -3′, *hus-1*: 5′-GGCAATC GACGTGTTTATCAAAAT -3′ and 5′- TCGTTTCGTGGATT-CATGCC -3′, *cep*-1: 5′- TGTCCAGAAAATGATAGACGGAGT -3′ and 5′-GCATCGGAAATCTTTGGCGT -3′, *egl-1*: 5′- ACACCCAAAACATTCA-CACCG -3′ and 5′- GGCAAAGGTGAGCA TCAGCA -3′, *ced-13*: 5′-TCGAGGGCAGAAAAACGTGA -3′ and 5′- ACAACAGCG GGAGAAAGTGT -3′, and *act-1*: 5′- AGACAATGGATCCGGAATGT -3′ and 5′- CATCC-CAGTTGGTGACGATA -3′. The sequences of *hus-1*, *cep-1*, *egl-1*, and *ced-13* primers were previously reported.[29] The thermal cycling condition comprised an initial denaturation step at 95 °C for 10 min, followed by 40 cycles of 95 °C for 15 s, 60 °C for 15 s and 72 °C for 30 s. The relative change in gene expression was analyzed using the $2^{-\Delta\Delta Ct}$ method, where each target gene's cycle threshold (C$_t$) values were normalized to *act-1* for controlling the variability in expression levels in *C. elegans*. Each treatment was performed in triplicate.

2.12. Measurement of C. elegans body length and brood size

To investigate the toxicity of the extracts on worm development, the body length of the worms was measured. L4 larval stage worm was individually sorted, and transferred onto different NGM containing *E. coli* OP50 supplemented with the treatment. The nematodes were allowed to grow for 24 h, and at least ten worms per treatment were then snapped and measured for the body length using Motic Images Plus 3.0 software. To investigate the effect of the extracts on fertility, the total number of eggs laid by each worm was counted and scored. L4 larval stage worm was individually sorted, and transferred onto different NGM containing *E. coli* OP50 supplemented with the extracts. The nematodes were allowed to grow and lay eggs at 20 °C. The adult worms were moved to new treatment plates every day. The eggs were observed under a dissecting microscope and were counted daily until the adult worm stopped laying eggs.

2.13. Molecular docking analysis

The molecular docking analysis was used to identify the potential active ingredients interacting with DAF-16 in each extract. The chemical constituents of the extracts were obtained from LC-MS data (Supplementary data 1). The selected candidate ligands were investigated for the binding affinity against the DAF-16 protein, following our previous study.[31] In brief, the 3D structure of the DAF-16 protein and the chemical structures of the compounds of interest were used for docking studies. The chemical structures of the reference drugs for DAF-16, Epigallocatechin gallate, and the metabolite constituents of the extracts were obtained from PubChem database.[32] The blind docking approach was employed to estimate the strong binding site of the molecules. The DockThor program was then used to calculate the binding affinities of the molecules against the target protein. It is a grid-based docking method which computes different binding modes of ligands on the protein structure.[33]

2.14. Statistical analysis

All experiments were carried out in at least three independent experiments. The Shapiro-Wilk test was used for normality testing. Statistical analyses were conducted using one-way analysis of variance (ANOVA), followed by Dunnett's multiple comparison test. For the lifespan assay, the statistical significance among different groups was determined by a log-rank (Mantel-Cox) test followed by the Gehan-Breslow-Wilcoxon test. Differences with $P < 0.05$ were considered statistically significant for all experiments.

3. Results

3.1. Glucan content of xLr® and its fractions

The glucan content in xLr® and its fractions were determined and shown in Fig. 1 xLr® consisted of 32.01 % (w/w) glucans. Among them, 19.86 % was determined to be α-glucan (w/w) and 12.14 % (w/w) was β-glucan. For the xLr® fractions, total glucan content found in HLR, MLR, and LLR were 32.40, 20.85, and 16.41 % (w/w), respectively. Interestingly, β-glucan content was found higher in HLR fraction (α: 19.86 % (w/w) and β: 12.54 % (w/w)), whereas MLR and LLR fractions had lower β-glucan (α: 18.12 % (w/w) and β: 2.72 % (w/w)) and (α: 16.22 % (w/w) and β: 0.27 % (w/w), respectively).

3.2. Phenolic and flavonoid contents of xLr® and its fractions

The total phenolic and flavonoid contents in xLr®, HLR, MLR, and LLR were determined and shown in Table 1. There is a statistical difference in the content of phenolics between xLr® and the fractions, whereas the difference was not found in the flavonoid content. The highest total phenolic content was xLr® (11.22 ± 0.09 mg GAE/g dry weight extract), followed by LLR, HLR, and MLR, respectively (9.68 ± 0.13, 4.30 ± 0.04, and 3.23 ± 0.04 mg GAE/g dry weight extract, respectively). Besides, MLR exhibited the highest total flavonoid content (5.62 ± 0.49 mg QE/g dry weight extract), followed by LLR, xLr®, and HLR, respectively (5.05 ± 0.19, 5.03 ± 0.34, and 4.79 ± 0.88 mg QE/g dry weight extract, respectively).

3.3. Free radical scavenging activity xLr® and its fractions

The ABTS radical scavenging activity of the extracts is presented in Table 2. At 1 mg/mL, xLr® exhibited ABTS scavenging activity of 93.82 ± 3.64 **%.** Among the xLr®'s fractions, LLR had the highest scavenging activity **(88.66 ± 3.19 %)** followed by HLR **(55.74 ± 2.56 %)** and MLR **(37.60 ± 2.15 %),** respectively**.** Interestingly, the level of free radical
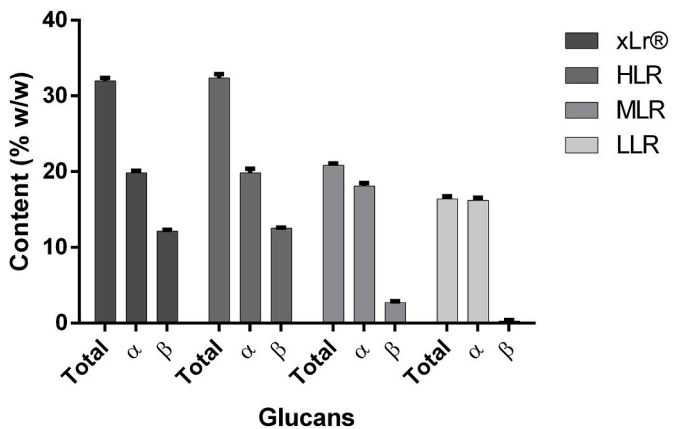
Fig. 1. Glucan content of xLr®, HLR, MLR and LLR. xLr® consists of both α and β glucans. Among the xLr® fractions, β glucan was higher in HLR, meanwhile β glucan is rarely detected in both MLR and LLR.

Table 1
Total phenolic and flavonoid contents of xLr® and its fractions.

Compound	Total phenolic content (mg GAE/g dry weight extract)	Total flavonoid content (mg QE/g dry weight extract)
xLr®	11.22 ± 0.09[1]	5.05 ± 0.19[1]
HLR	4.30 ± 0.04[2]	4.79 ± 0.88[1]
MLR	3.23 ± 0.04[3]	5.62 ± 0.49[1]
LLR	9.68 ± 0.13[4]	5.03 ± 0.34[1]

Data presents as mean ± SEM; different superscript numbers equal to significant difference.

Table 2
Free radical scavenging activity of xLr® and its fractions using ABTS assay.

Extract/fraction/compound	Scavenging activity	
	Percentage (%)	EC$_{50}$ (µg/mL)
xLr® (1 mg/mL)	93.82 ± 3.64	283.91 ± 24.67
HLR (1 mg/mL)	55.74 ± 2.56	889.73 ± 49.52
MLR (1 mg/mL)	37.60 ± 2.15	>1000
LLR (1 mg/mL)	88.66 ± 3.19	365.82 ± 25.16
Ascorbic acid (10 µg/mL)	99.11 ± 0.21	3.56 ± 0.11

Data presents as mean ± SEM.

scavenging activity was correlated with the level of phenolic content in each extract or fraction.

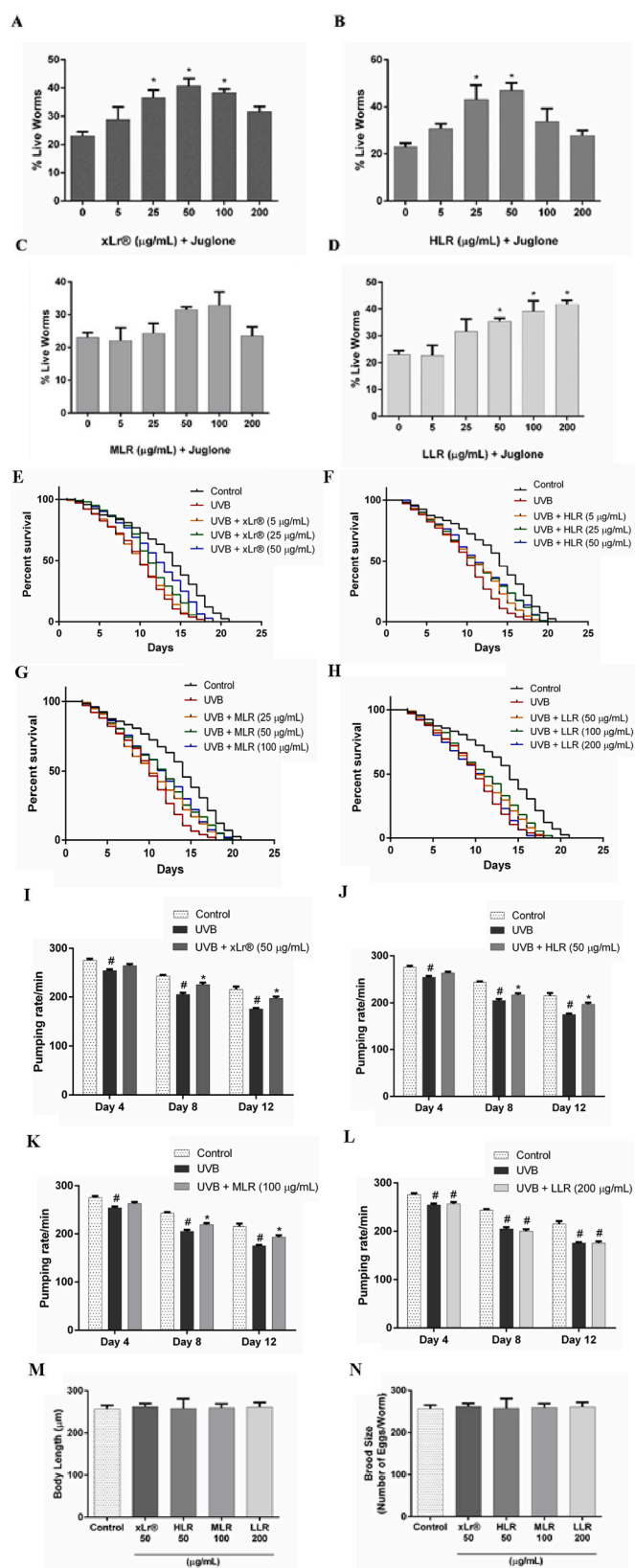### 3.4. xLr® and its fractions protect C. elegans against juglone-induced stress

The worm survival rate was significantly increased at concentrations of 25, 50, and 100 µg/mL in xLr®; 25 and 50 µg/mL in HLR; and 50, 100, and 200 µg/mL in LLR (Fig. 2A, B, and 2D). In contrast, MLR slightly increased survival percentage without significance at the concentrations of 50 and 100 µg/mL, when compared to their respective control group (Fig. 2C).

3.5. xLr® and its fractions ameliorate C. elegans lifespan under UVB irradiation

To determine whether xLr® and its fractions were able to protect *C. elegans* against UVB radiation, the lifespan of *C. elegans* treated with xLr® and its fractions: HLR, MLR, and LLR, exposed to UVB radiation of 100 J/cm^2 were analyzed against untreated worms (Fig. 2E–H and Table 3). Among the tested concentrations of each extract, 50 µg/mL of xLr® could increase mean lifespan by 18.58 % and increase maximum lifespan by up to 16.46 % when compared to worms exposed to UVB without treatment. HLR at 50 µg/mL significantly increased the mean and maximum lifespans to 14.01 % and 22.34 %, respectively, compared to worms exposed to UVB without treatment. MLR at 100 µg/mL significantly increased the mean and maximum lifespans of the worms by 14.82 % and 20.25 %, respectively, when compared to worms exposed to UVB without treatment.

3.6. xLr® and its fractions improve healthspan in UVB-irradiated C. elegans

Pharyngeal pumping reveals age-related decline of muscle function, rendering it a marker for healthspan and aging. UVB-exposed *C. elegans* significantly decreased pumping rate measured from day 4 to day 12. Consistent with the lifespan assay, *C. elegans* treated with xLr® and its fractions (HLR and MLR) significantly reversed the pharyngeal pumping rate after UVB radiation (100 J/cm^2) compared to worms exposed to UVB without treatment. However, the fraction LLR showed no significant difference (Fig. 2I–L).

Fig. 2. The effects of xLr® and its fractions in *C. elegans* model. Anti-oxidative stress activity against juglone induction in *C. elegans*. Percentage of survival worm in the co-treatment of juglone (80 μM) and xLr® and its fractions: (**A**) xLr®, (**B**) HLR, (**C**) MLR, and (**D**) LLR for 24 h. The effect of xLr® and its fractions on *C. elegans* lifespan extension under UVB induction. The percentage of survival worms after exposure to UVB in the presence or absence of (**E**) xLr®, (**F**) HLR, (**G**) MLR, and (**H**) LLR extracts. The effects of xLr® and its fractions on age-related decline pharyngeal pumping of *C. elegans* under UVB induction. The pharyngeal pumping rate of the worms after exposure to UVB in the presence or absence of (**I**) xLr®, (**J**) HLR, (**K**) MLR, and (**L**) LLR extracts. The effects of xLr® and its fractions on (**M**) body length and (**N**) brood size of *C. elegans*. All data are shown as the mean ± SEM of triplicate values. Statistical significance was analyzed by a One-way ANOVA and Dunnett's *post hoc* test. For lifespan assay, statistical significance was analyzed by a log-rank (Mantel − Cox) test followed by the Gehan-Breslow-Wilcoxon test.

3.7. Body length and brood size of C. elegans are not altered by xLr® and its fractions

To analyze the impact of the extracts on the overall development and reproduction of *C. elegans*, the body length and brood size of the worms were measured after treatment with the highest effective doses of xLr® and its fractions that showed significant survival rates. Analyses of the body length revealed no difference in mean length per worm when treated with xLr® and its fractions compared to the untreated control group (Fig. 2M). Moreover, the treatment with xLr® and its fractions did not affect the reproductive health of the worms when compared to the untreated control group (Fig. 2N).

3.8. xLr® and its fractions affect anti-oxidant and apoptosis-related mRNA expressions in UVB-exposed C. elegans

To investigate the anti-oxidant effect of xLr® and its fractions in response to UVB exposure, the regulation of expression of *daf-16* and *sod-3,* which are the important regulators that trigger anti-oxidant and anti-aging responses in *C. elegans*, were analyzed through the real-time quantitative RT-PCR. Both *daf-16* and *sod-3* gene expression in the worms exposed to UVB treated with xLr® and its fractions were found to be significantly up-regulated when compared to worms exposed to UVB without treatment (Fig. 3A and B). xLr® and its fractions HLR and MLR significantly down-regulated *cep-1*, *hus-1*, *ced-13*, and *egl-1* expression in treated worms when compared to untreated worms. Whereas the LLR fraction did not show such effects (Fig. 3C–E).

3.9. xLr® and its fractions decrease intracellular ROS production in UVB-exposed C. elegans

To investigate the impact of xLr® and its fractions on UVB-induced ROS, DCFH-DA was used to analyze the intracellular ROS. The data showed a significant reduction in ROS in *C. elegans* treatment with xLr® and HLR compared to UVB-exposed *C. elegans*. MLR fraction also showed a reduction in intracellular ROS but was not significant, and LLR fraction did not show any change compared to untreated UVB-exposed *C. elegans* (Fig. 4A).

3.10. xLr® and its fractions up-regulate DAF-16 translocation and SOD-3 activation in UVB-exposed C. elegans

DAF-16 is an important regulator of the insulin signaling pathway and regulates stress responses in *C. elegans*. The TJ356 mutant *C. elegans* containing GFP reporter of DAF-16 was used for studying DAF-16 nuclear translocation in *C. elegans*. The effect of xLr® and its fractions on the DAF-16 nuclear translocation after UVB irradiation was analyzed. The treatment with xLr® and LLR showed a significant increase in nuclear translocation in the worms, whereas MLR and HLR did not increase the translocation when compared to UVB-exposed untreated *C. elegans*,

Table 3
Effect of LR on *C. elegans* lifespan after UVB exposure.

Extract (μg/mL)		Mean lifespan		Maximum lifespan		P value of	Number
		(day) ± SEM	% increase (vs. UVB)	(day) ± SEM	% increase (vs. UVB)	lifespan (vs. UVB)	of worms
Control		13.20 ± 0.46	–	20.60 ± 0.24	–	–	120
UVB		9.85 ± 0.39	–	15.80 ± 0.91	–	–	101
UVB + xLr®	5	9.97 ± 0.40	1.12	17.00 ± 0.58	7.59	0.8809	102
	25	11.23 ± 0.37	14.01	17.40 ± 0.25	10.13	0.0167 (ª)	102
	50	11.68 ± 0.42	18.58	18.40 ± 0.24	16.46	0.0006 (ª)	100
UVB + HLR	5	10.70 ± 0.44	8.63	18.00 ± 0.37	13.92	0.1423	105
	25	11.10 ± 0.46	11.32	19.20 ± 0.20	21.52	0.0671	110
	50	11.23 ± 0.48	14.01	19.33 ± 0.33	22.34	0.0311 (ª)	103
UVB + MLR	25	10.47 ± 0.44	6.29	17.67 ± 0.17	11.84	0.4044	101
	50	11.22 ± 0.44	13.91	19.25 ± 0.25	21.84	0.0259 (ª)	116
	100	11.31 ± 0.46	14.82	19.00 ± 0.45	20.25	0.0209 (ª)	103
UVB + LLR	50	10.42 ± 0.41	5.78	17.60 ± 0.24	11.39	0.3571	108
	100	10.66 ± 0.43	8.22	18.67 ± 0.33	18.16	0.0834	113
	200	9.97 ± 0.39	1.22	16.75 ± 0.25	6.01	0.7525	111

Statistical significance was analyzed by a log-rank (Mantel − Cox) test followed by the Gehan-Breslow-Wilcoxon test.
  [a] $P < 0.05$.

although the total mRNA expression of DAF-16 was found to be increased in all the treatment groups (Fig. 4B). Further, the expression of the downstream target gene SOD-3 was also analyzed using transgenic *C. elegans* strain CF1553 containing GFP reporter of SOD-3. The SOD-3: GFP expression of *C. elegans* treated with xLr® and its fractions was found to be significantly increased compared to control and UVB-exposed worms (Fig. 4C). These results suggest that a synergistic activity of the various fractions of xLr® induces a protective effect against UVB through DAF-16 regulation.

3.11. Potential active metabolites activating DAF-16 protein are identified using docking study

The chemical constituents of xLr® and its fractions were identified using LC/MS as shown in Supplementary data 1. The candidates from each fraction were further investigated the binding potential to DAF-16 protein for identifying the possible active ingredients in this matter using the molecular docking study. The docking results were shown in Table 4. The docking score expressed the binding energy as Gibbs free energy by which the compounds displayed lower binding energy were considered better.[34] The well-known natural occurring DAF-16 activator, epigallocatechin gallate in which used as the reference compound, exhibited the docking score at −7.53 kcal/mol. Among the xLr®-identified compounds, ajmaline exhibited the lowest docking score (−9.16 kcal/mol), followed by 4-caffeoylquinic acid (−8.89 kcal/mol). Obtusaquinone (−8.14 kcal/mol), Coniine (−8.00 kcal/mol), and Curcumin (−8.66 kcal/mol) showed the lowest binding energy in HLR, MLR, and LLR, respectively. Meanwhile butyl lactate (−6.82 kcal/mol), neochlorogenic acid (−7.90 kcal/mol), and carnitine (−7.76 kcal/mol) were the second ranked of the lowest docking score from HLR, MLR, and LLR, respectively.

4. Discussion

Aging is influenced by several factors, including genetics, metabolic processes, and environmental exposure.[35] The influence of the environment, especially UV radiation, is one of the critical factors leading to skin aging.[36] Skin aging due to UV exposure (also known as photoaging) runs in tandem with the chronological aging of human skin.[35] UV radiation, especially UVB, can cause a variety of cellular responses, including cell damage, inflammation, and apoptosis.[37,38] Exposure to UVB leads to collagen degradation, followed by ROS production, which results in photoaging.[39] Several studies have been conducted to search for new products from natural sources that contain compounds that have protective effects to prevent damaging effects caused by UV on skin cells.[40,41]

Lignosus rhinocerus (Cooke) Ryvarden, or commonly known as tiger milk mushroom is traditionally used to treat asthma, cough, fever, food poisoning, and wounds.[42] The present study investigated the extract of TM02® cultivar, named xLr® and its respective high (HLR), medium (MLR) and low (LLR) molecular weight fractions. We explored its ability to attenuate UVB-induced damage and photoaging in *C. elegans*.

β-glucan exhibits a variety of therapeutically important properties and is the major constituent of mushroom cell wall.[43] A recent study reported that dietary uptake of β-glucan can promote anti-oxidant activity and delay the onset of age-related biomarkers in aged fish.[44] Total glucan analysis, among the xlr® fractions, HLR was found to contain higher glucan content rich in both α- and β-glucan, followed by MLR and LLR which have the least content of β-glucan. Additionally, the total phenolic and flavonoid content was also analyzed, xLr® was found to be rich in total phenolic content. LLR was found to have the highest phenolic content amongst the fractions. On the other hand, the flavonoid content was highest in MLR followed by LLR, xLr® and HLR. *In vitro* analysis revealed significantly high free radical scavenging capacity exhibited by xLr®. Studies have established the anti-oxidant capacity of phenolic and flavonoid compounds derived from natural sources. These compounds are known to inhibit membrane damage by scavenging free radicals that induce lipid peroxidation and DNA damage.[45]

The preliminary study to analyze the anti-oxidant and protective activity against UVB exposure, xLr® and its fractions showed a significant increase in the survival rate of *C. elegans* treated against juglone-induced oxidative stress. This could be attributed to the free radical scavenging activity of the extracts, which makes it a potent source of anti-oxidants. Hence, the highest concentrations were taken for further studies. xLr® and its fractions, specifically HLR and MLR, significantly prolonged the lifespan and increased mean and maximum survival days of UVB-irradiated *C. elegans*. These results indicate that xLr® significantly improved the stress resistance of *C. elegans* and counteracted UVB-induced photoaging. Interestingly, different fractions from xLr® exhibited different effects in juglone-mediated and UVB-induced oxidative stress. These activities may be affected by the different compounds found in each fraction. Notably, according to the juglone-induced toxicity assay, xLr® and HLR fraction at high concentrations (200 μg/mL for xLr®, and 100–200 μg/mL for HLR) failed to recuse the worms from oxidative stress. It has been elucidated that some bioactive compounds have beneficial anti-oxidant properties at lower doses, and have potential toxicity at higher doses.[7] It is possible that these compounds may be dominant in HLR fraction.

To investigate the underlying mechanism of the anti-oxidant effect, DAF-16/FOXO pathway was investigated. Under normal circumstances, DAF-16 activation is responsible for stress response and lifespan extension.[46] Upon its activation, DAF-16 induces the transcription of several

A

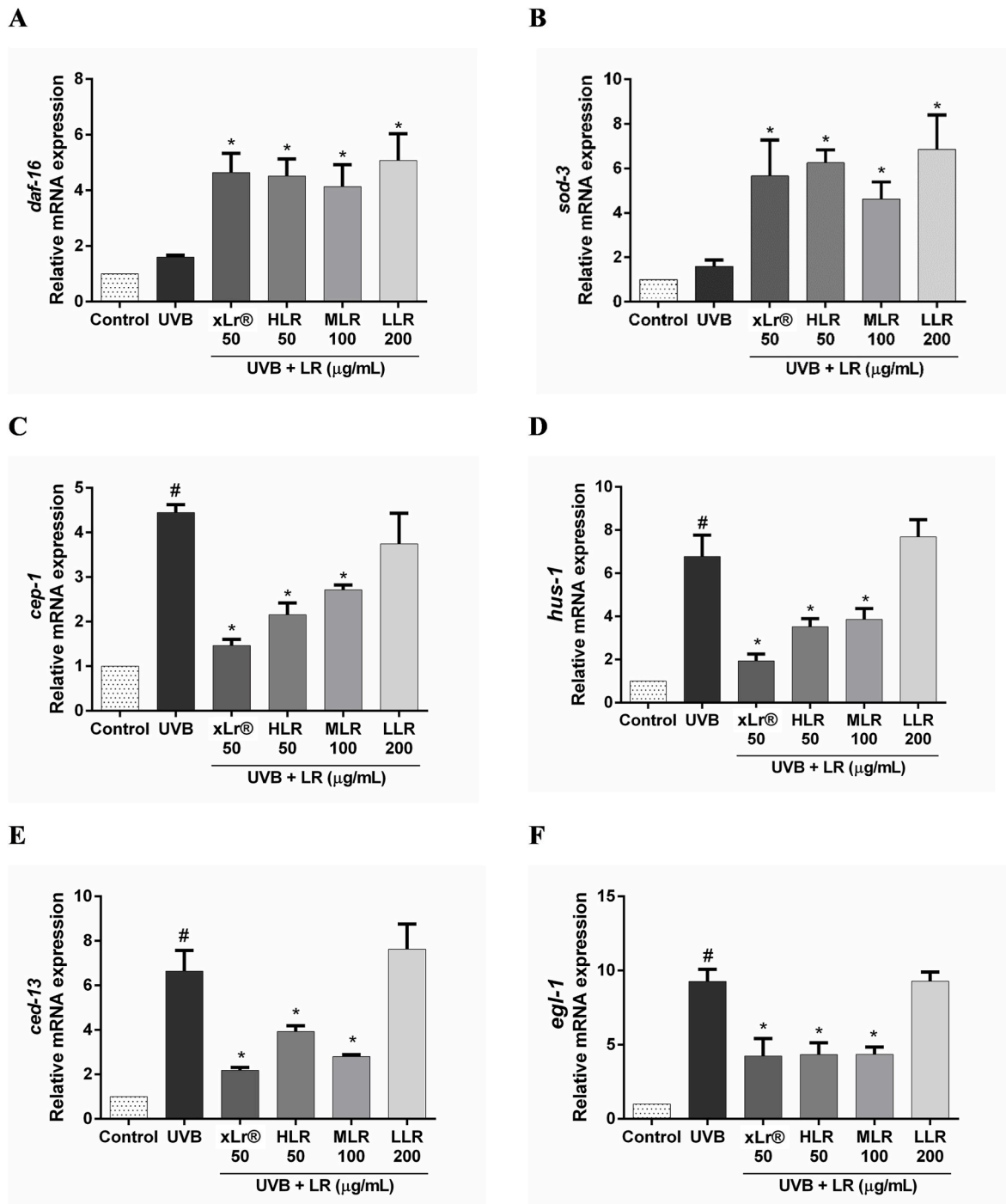**B**

C

D

E

F

Fig. 3. Real-time qRT-PCR analysis of anti-oxidant and apoptosis-related gene expressions in UVB-exposed *C. elegans*. The level of mRNA expression of anti-oxidant-related genes: (**A**) *daf-16* and (**B**) *sod-3* in UVB-exposed *C. elegans* in the presence or absence of LR extracts. The level of mRNA expression of apoptosis-related genes: (**C**) *cep-1*, (**D**) *hus-1*, (**E**) *ced-13*, (**F**) *egl-1* in UVB-exposed *C. elegans* in the presence or absence of xLr® and its fractions. All data are shown as the mean ± SEM of triplicate values. Statistical significance was analyzed by a One-way ANOVA and Dunnett's *post hoc* test. #$p < 0.05$ vs control group, *$p < 0.05$ vs UVB group.

genes involved in the anti-oxidative network, such as SOD-3, which encodes mitochondrial superoxide dismutase (Mn-SOD). Previous studies have been suggested that this enzyme could eliminate free radicals and protect the worms against oxidative stress.[47] In the present study, we observed a significant increase in *daf-16* and *sod-3* expression in worms after treatment with xLr® and its fractions HLR, MLR, and LLR when compared to untreated UVB-exposed *C. elegans*. These results suggest that xLr® and its fractions may exert their anti-oxidant effect possibly through the activation of the DAF-16/FOXO pathway.

Furthermore, the nuclear translocation of DAF-16 was also analyzed using transgenic strain TJ356. Treatment with xLr® and LLR showed an increase in DAF-16 translocation to the nucleus in UVB-exposed worms, whereas no significant changes were observed in MLR and HLR fractions compared to untreated UVB-exposed *C. elegans*. Interestingly, the downstream player of DAF-16, SOD-3 was found to be expressed significantly higher in treatment groups xLr®, HLR, MLR, and LLR when compared to UVB-exposed *C. elegans*.

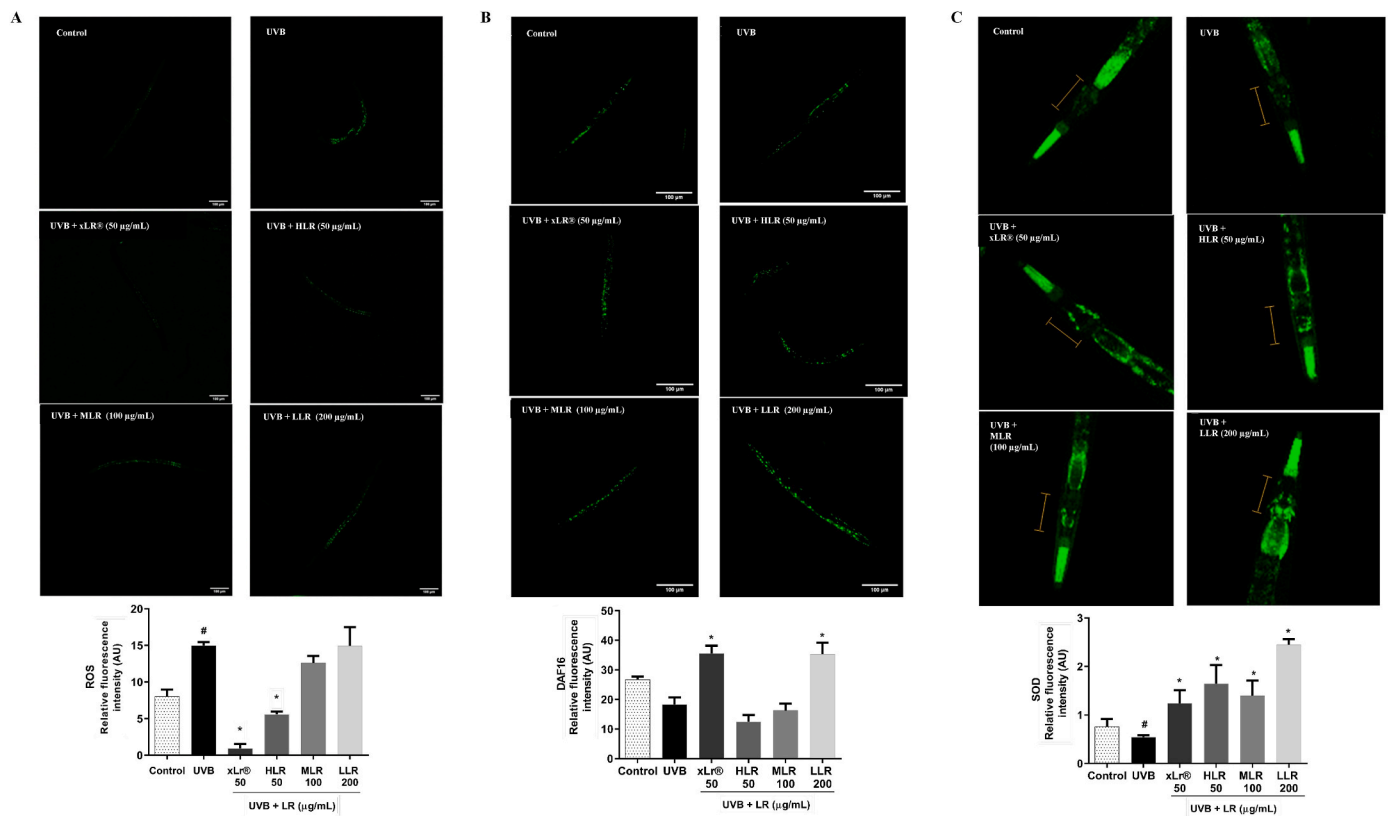Studies show that UV causes cell death through the activation of

Fig. 4. (**A**) The effect of xLr® and its fractions on intracellular ROS in UVB-exposed *C. elegans*. (**B**) The effect of xLr® and its fractions on nuclear translocation of DAF-16 in UVB-exposed *C. elegans*. (**C**) The effect of xLr® and its fractions on the expression of SOD-3 in UVB-exposed *C. elegans*. For SOD-3, the relative fluorescence intensity was analyzed at the pharyngeal region (analyzed area marked with bar). A whole body image was taken and the pharyngeal region was cropped for observation and analysis of SOD-3:GFP expression. Scale bar 100 μm. Statistical significance was analyzed by a One-way ANOVA and Dunnett's *post hoc* test. $\#p < 0.05$ vs control group, $*p < 0.05$ vs UVB group.

apoptosis.[48] The UV-mediated apoptosis process involves several different molecular pathways, including DNA damage.[48] In *C. elegans*, several apoptosis-related genes are up-regulated after UVB exposure.[29] UVB exposure can activate CEP-1, a P53 homolog in *C. elegans*.[49] These can further induce the activation of EGL-1 and CED-13, which are BH3-only proteins and are known to interact with CED-9 (a pro-apoptotic protein). Overexpression of EGl-1 reportedly results in triggering the apoptosis pathway.[49,50] HUS-1 is a nuclear protein *C. elegans* and mediates apoptosis through CEP-1, followed by the EGL-1 mechanism.[51] The results of qRT-PCR showed that the worm treated with xLr®, HLR, and MLR groups but not LLR, could significantly attenuate the increase in expression levels of *hus-1*, *cep-1*, *egl-1* and *ced-13* caused by UVB, which explained their mechanism of inhibiting apoptosis and prolonging lifespan. Notably, although stress resistance activity *via* the DAF-16/FOXO pathway was marked, failure to abolish apoptosis by LLR rendered it ineffective in attenuating UVB-induced photoaging in *C. elegans*.
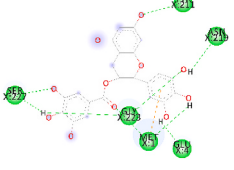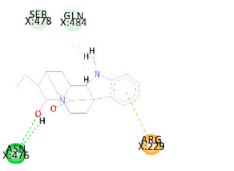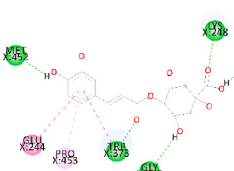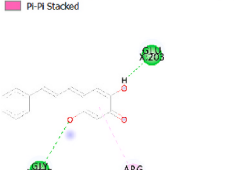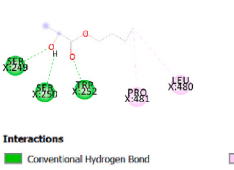
According to our results, the chemical constituents of each fraction, including glucan, phenolic, flavonoid, were semi-quantitative measured and found the difference between each fraction. Furthermore, the small molecules in each extract were identified using LC/MS and investigated for the potential interacting compounds to the DAF-16 protein using molecular docking analysis. The best potential bioactive candidates from xLr®, HLR, MLR, and LLR were ajmaline, butyl lactate, neochlorogenic acid, and carnitine, respectively. Interestingly, these compounds exhibited lower binding energy compared to epigallocatechin gallate, the standard agonists of DAF-16 activator. However, the docking studies often rely on simplified models of proteins and ligands that may not fully represent the complexity of biological systems.[52] Further experiments of these potential compounds are necessary to validate their
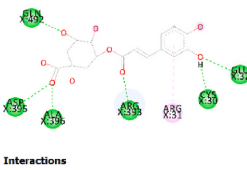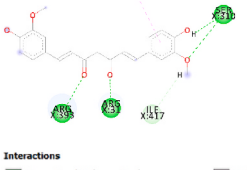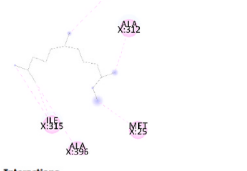
activity.

Our current study suggests the possibility of synergistic or additive effect between HLR, MLR and LLR fractions of xLr® in the protective activity against UVB induced oxidative stress. However, among the xLr® fractions, HLR was identified as the most potent fraction, potentially due to the presence of β-glucan as a major active ingredient when compared to another fractions. This aligns with research indicating that β-glucan possesses UV-protective properties, which may help in mitigating photoaging effects.[53,54] Besides, in agreement with previous study, the anti-inflammatory property of xLr® was mainly contributed by its high molecular weight fraction, and the possibility of synergistic effect between all three fractions should be further elucidated.[26]

Tiger milk mushroom has been studied for its potential anti-oxidant, anti-inflammatory, and immunomodulatory because it is rich in the composition of bioactive compounds, including polysaccharides, phenolics, flavonoids, and terpenoids.[55–57] These properties of the bioactive ingredients contribute to health benefits, particularly beneficial for protecting the skin against UV-induced damage and other environmental stressors.[58,59] This mushroom has shown promising photoprotective activities against UVB-induced damage. The methanol extract has processed the promising photoprotective activities against UV-induced damage in human keratinocyte HaCaT cells.[60] The protective effect is associated with the upregulation of anti-apoptotic proteins like BCL-XL and BCL-2, which help in preventing programmed cell death.[60] In addition, the tiger milk mushroom has possessed beneficial effects to the skin. Cold water extract of the mushroom can help prevent skin aging and maintain healthy skin by inhibiting melanin production at the intra- and extracellular levels of B16-F1 melanoma cells and upregulating the production of procollagen type 1 in HaCaT cells.[61] Taken together, our findings highlight and support the significant

Table 4

The molecular docking results of the potential candidates from xLr® and its fractions to interact with DAF-16 protein.

Compound		Docking Score (kcal/mol)	DAF-16 and ligand interaction
Epigallocatechin gallate		−7.53	
xLr®	Ajmaline	−9.16	
	4-Caffeoylquinic acid	−8.89	
HLR	Obtusaquinone	−8.14	
	Butyl lactate	−6.82	
MLR	Coniine	−8.00	

Table 4 (*continued*)

Compound		Docking Score (kcal/mol)	DAF-16 and ligand interaction
	Neochlorogenic acid	−7.90	
LLR	Curcumin	−8.66	
	Carnitine	−7.76	

implications for photoprotective effects of xLr® and its fractions against UVB irradiation that could be beneficial for the development of anti-UV products.

5. Conclusions

The *in vivo* studies exhibited that xLr® and its fractions could enhance the stress resistance of the UVB-exposed *C. elegans via* the regulation of oxidative stress and apoptotic pathways. Hence, the current findings revealed the protective activities and their possible molecular mechanisms responsible for the anti-photoaging effects of the tiger milk mushroom and its fractions. These results suggest that tiger milk mushroom is a natural resource that can ameliorate UVB damage and has the potential to be included as efficacious content in innovative skin care products.

Declaration of competing interest

The authors declare that they have no known competing financial interests or personal relationships that could have appeared to influence the work reported in this paper.

Appendix A. Supplementary data

Supplementary data to this article can be found online at https://doi.org/10.1016/j.jtcme.2024.11.004.

References

1. Addor FAS. Beyond photoaging: additional factors involved in the process of skin aging. *Clin Cosmet Invest Dermatol.* 2018;11:437–443.
2. Svobodova A, Walterova D, Vostalova J. Ultraviolet light induced alteration to the skin. *Biomed Pap Med Fac Univ Palacky Olomouc Czech Repub.* 2006;150(1):25–38.
3. de Gruijl FR. Photocarcinogenesis: UVA vs UVB. *Methods Enzymol.* 2000;319:359–366.
4. D'Orazio J, Jarrett S, Amaro-Ortiz A, Scott T. UV radiation and the skin. *Int J Mol Sci.* 2013;14(6):12222–12248.
5. Arulselvan P, Fard MT, Tan WS, et al. Role of antioxidants and natural products in inflammation. *Oxid Med Cell Longev.* 2016;2016, 5276130.
6. Hahn D, Shin SH, Bae JS. Natural antioxidant and anti-inflammatory compounds in foodstuff or medicinal herbs inducing heme oxygenase-1 expression. *Antioxidants.* 2020;9(12).
7. Samtiya M, Aluko RE, Dhewa T, Moreno-Rojas JM. Potential health benefits of plant food-derived bioactive components: an overview. *Foods.* 2021;10(4).
8. Rodríguez-Yoldi MJ. Anti-inflammatory and antioxidant properties of plant extracts. *Antioxidants.* 2021;10(6).
9. Lai WH, Siti Murni MJ, Fauzi D, Abas Mazni O, Saleh NM. Optimal culture conditions for mycelial growth of Lignosus rhinocerus. *MYCOBIOLOGY.* 2011;39(2):92–95.
10. Jamil NAM, Rashid NMN, Abd Hamid MH, Rahmad N, Al-Obaidi JRJ. Biotechnology. Comparative nutritional and mycochemical contents, biological activities and LC/MS screening of tuber from new recipe cultivation technique with wild type tuber of tiger's milk mushroom of species Lignosus rhinocerus. 2018;34(1):1–10.
11. Yap YH, Tan N, Fung S, et al. Nutrient composition, antioxidant properties, and anti-proliferative activity of Lignosus rhinocerus Cooke sclerotium. 2013;93(12):2945–2952.
12. Nallathamby N, Serm LG, Raman J, et al. Identification and in vitro evaluation of lipids from sclerotia of Lignosus rhinocerotis for antioxidant and anti-neuroinflammatory activities. 2016;11(10), 1934578X1601101016.
13. Wong YE, Razif MFM, Ng ST, Tan CS, Fung SY, Murugan DD. Medicinal tiger milk mushroom Lignosus rhinocerus TM02® (agaricomycetes) sclerotia supplementation mitigates hypertension and alleviates vascular dysfunction partly through oxidative stress modulation in spontaneously hypertensive rats. *Int J Med Mushrooms.* 2024;26(11):27–40.
14. Yap C-SA, Razif MFM, Ng S-T, Tan C-S, Abd Jamil AH, Fung S-Y. Anti-oxidative effects of functional food, Lignosus rhinocerus scleroria (TM02® cultivar) using a type 2 diabetes mellitus rodent model. *Food Biosci.* 2022;49, 101944.
15. Baskaran A. *Suppression of Lipopolysaccharide and Hydrogen Peroxide-Induced Inflammatory Responses in Raw 264.7 Macrophage by Pleurotus Giganteus and Lignosus Rhinocerotis/Asweni A/p Baskaran.* 2015.
16. Suziana Zaila C, Farida Zuraina M, Norfazlina M, et al. *Antiproliferative effect of Lignosus rhinocerotis, the Tiger Milk Mushroom on HCT 116 human colorectal cancer cells. The Open Conference Proceedings Journal.* 2013. Paper presented at:.
17. Lai CK, Wong K-H, Cheung P. Antiproliferative effects of sclerotial polysaccharides from Polyporus rhinocerus Cooke (Aphyllophoromycetideae) on different kinds of leukemic cells 2008;10(3).
18. Lau BF, Abdullah N, Aminudin N, Lee HBJ. Chemical composition and cellular toxicity of ethnobotanical-based hot and cold aqueous preparations of the tiger's milk mushroom. *Lignosus rhinocerotis).* 2013;150(1):252–262.
19. Ng MJ, Kong BH, Teoh KH, et al. In vivo anti-tumor activity of Lignosus rhinocerus TM02® using a MCF7-xenograft NCr nude mice model. *J Ethnopharmacol.* 2023;304, 115957.
20. Yap HYY, Kong BH, Yap CSA, et al. Immunomodulatory effect and an intervention of TNF signalling leading to apoptotic and cell cycle arrest on ORL-204 oral cancer cells by tiger milk mushroom, Lignosus rhinocerus. *Food Technol Biotechnol.* 2022;60(1):80–88.
21. Mohanarji S, Dharmalingam S, Kalusalingam AJJoP, Sciences© B. Screening of Lignosus rhinocerus extracts as antimicrobial agents against selected human pathogens. 2012;18(18).
22. Ellan K, Thayan R, Raman J, Hidari KIPJ, Ismail N, Sabaratnam V. Anti-viral activity of culinary and medicinal mushroom extracts against dengue virus serotype 2: an in-vitro study. *BMC Compl Alternative Med.* 2019;19(1), 260-260.
23. Sillapachaiyaporn C, Chuchawankul S. HIV-1 protease and reverse transcriptase inhibition by tiger milk mushroom (Lignosus rhinocerus) sclerotium extracts: in
24. vitro and in silico studies. *Journal of traditional and complementary medicine.* 2020;10(4):396–404.
25. Goh N-Y, Yap YH-Y, Ng CL, et al. Water-soluble compounds from Lignosus rhinocerus TM02® (xLr™) modulate ACE2 activity and inhibit its interaction with SARS-CoV-2 spike-protein. *Food Biosci.* 2024;59, 104232.
26. Kittimongkolsuk P, Roxo M, Li H, Chuchawankul S, Wink M, Tencomnao T. Extracts of the tiger milk mushroom (Lignosus rhinocerus) enhance stress resistance and extend lifespan in Caenorhabditis elegans via the DAF-16/FoxO signaling pathway. 2021;14(2):93.
27. Lee SS, Tan NH, Fung SY, Sim SM, Tan CS, Ng ST. Anti-inflammatory effect of the sclerotium of Lignosus rhinocerotis (cooke) ryvarden, the tiger milk mushroom. *BMC Compl Alternative Med.* 2014;14:359.
28. Tan CS, Ng ST, Vikineswary S, Lo FP, Tee CS. Genetic markers for identification of a MALAYSIAN medicinal mushroom. *LIGNOSUS RHINOCERUS (CENDAWAN SUSU RIMAU).* 2010.
29. Rangsinth P, Prasansuklab A, Duangjan C, et al. Leaf extract of Caesalpinia mimosoides enhances oxidative stress resistance and prolongs lifespan in Caenorhabditis elegans. *BMC Compl Alternative Med.* 2019;19(1):164.
30. Li SM, Liu D, Liu YL, Liu B, Chen XH. Quercetin and its mixture increase the stress resistance of Caenorhabditis elegans to UV-B. *Int J Environ Res Publ Health.* 2020;17(5).
31. Pattarachotanant N, Sornkaew N, Warayanon W, et al. Aquilaria crassna leaf extract ameliorates glucose-induced neurotoxicity in vitro and improves lifespan in Caenorhabditis elegans. *Nutrients.* 2022;14(17).
32. Sharika R, Verma K, Tencomnao T, Chuchawankul S. Auricularia polytricha extract exerts SKN-1 and DAF-16 mediated longevity and stress resistance against UV-B exposure in Caenorhabditis elegans. *Nutr Healthy Aging.*
33. Wang Y, Xiao J, Suzek TO, Zhang J, Wang J, Bryant SH. PubChem: a public information system for analyzing bioactivities of small molecules. *Nucleic Acids Res.* 2009;37(suppl_2):W623–W633.
34. Guedes IA, Costa LSC, Dos Santos KB, et al. Drug design and repurposing with DockThor-VS web server focusing on SARS-CoV-2 therapeutic targets and their non-synonym variants. *Sci Rep.* 2021;11(1):5543.
35. Gibbs JWJToCAoA, Sciences. *A Method of Geometrical Representation of the Thermodynamic Properties by Means of Surfaces.* 1873:382–404.
36. Rittié L, Fisher GJ. UV-light-induced signal cascades and skin aging. *Ageing Res Rev.* 2002;1(4):705–720.
37. Kim HK. Protective effect of garlic on cellular senescence in UVB-exposed HaCaT human keratinocytes. *Nutrients.* 2016;8(8).
38. Lee CH, Wu SB, Hong CH, Yu HS, Wei YH. Molecular mechanisms of UV-induced apoptosis and its effects on skin residential cells: the implication in UV-based phototherapy. *Int J Mol Sci.* 2013;14(3):6414–6435.
39. Caricchio R, McPhie L, Cohen PL. Ultraviolet B radiation-induced cell death: critical role of ultraviolet dose in inflammation and lupus autoantigen redistribution. *J Immunol.* 2003;171(11):5778–5786.
40. Wang F, Smith NR, Tran BA, Kang S, Voorhees JJ, Fisher GJ. Dermal damage promoted by repeated low-level UV-A1 exposure despite tanning response in human skin. *JAMA Dermatol.* 2014;150(4):401–406.
41. Svobodová A, Vostálová J. Solar radiation induced skin damage: review of protective and preventive options. *Int J Radiat Biol.* 2010;86(12):999–1030.
42. Kostyuk V, Potapovich A, Albuhaydar AR, Mayer W, De Luca C, Korkina L. Natural substances for prevention of skin photoaging: screening systems in the development of sunscreen and rejuvenation cosmetics. *Rejuvenation Res.* 2018;21(2):91–101.
43. Lai WH, Siti Murni MJ, Fauzi D, Abas Mazni O, Saleh NM. Optimal culture conditions for mycelial growth of Lignosus rhinocerus. *MYCOBIOLOGY.* 2011;39(2):92–95.
44. Bak WC, Park JH, Park YA, Ka KH. Determination of glucan contents in the fruiting bodies and mycelia of lentinula edodes cultivars. *MYCOBIOLOGY.* 2014;42(3):301–304.
45. Song L, Zhou Y, Ni S, et al. Dietary intake of β-glucans can prolong lifespan and exert an antioxidant action on aged fish nothobranchius guentheri. *Rejuvenation Res.* 2020;23(4):293–301.
46. Rani R, Arora S, Kaur J, Manhas RK. Phenolic compounds as antioxidants and chemopreventive drugs from Streptomyces cellulosae strain TES17 isolated from rhizosphere of Camellia sinensis. *BMC Compl Alternative Med.* 2018;18(1):82.
47. Mukhopadhyay A, Oh SW, Tissenbaum HA. Worming pathways to and from DAF-16/FOXO. *Exp Gerontol.* 2006;41(10):928–934.
48. McElwee J, Bubb K, Thomas JH. Transcriptional outputs of the Caenorhabditis elegans forkhead protein DAF-16. *Aging Cell.* 2003;2(2):111–121.
49. Kulms D, Schwarz T. Molecular mechanisms of UV-induced apoptosis. *Photodermatol Photoimmunol Photomed.* 2000;16(5):195–201.
50. Stergiou L, Doukoumetzidis K, Sendoel A, Hengartner MO. The nucleotide excision repair pathway is required for UV-C-induced apoptosis in Caenorhabditis elegans. *Cell Death Differ.* 2007;14(6):1129–1138.
51. Nehme R, Conradt B. egl-1: a key activator of apoptotic cell death in C. elegans. *Oncogene.* 2008;27(Suppl 1):S30–S40.
52. Hofmann ER, Milstein S, Boulton SJ, et al. Caenorhabditis elegans HUS-1 is a DNA damage checkpoint protein required for genome stability and EGL-1-mediated apoptosis. *Curr Biol.* 2002;12(22):1908–1918.
53. Pattarachotanant N, Sukjamnong S, Rangsinth P, et al. Caenorhabditis elegans extract exerts neuroprotective effect against benzo [a] pyrene-induced toxicity in human SH-SY5Y cells: an RNA-seq-based transcriptome analysis. *Nutrients.* 2024;16(16):2727.
54. da Silva AF, Oliveira RJ, Niwa AM, D'Epiro GF, Ribeiro LR, Mantovani MS. Anticlastogenic effect of β-glucan, extracted from Saccharomyces cerevisiae, on cultured cells exposed to ultraviolet radiation. *Cytotechnology.* 2013;65(1):41–48.

54. Schiano I, Raco S, Cestone E, Jesenak M, Rennerova Z, Majtan J. Pleuran-β-Glucan from oyster culinary-medicinal mushroom, pleurotus ostreatus (agaricomycetes), soothes and improves skin parameters. *Int J Med Mushrooms.* 2021;23(12):75–83.
55. Fung S-Y, Tan C-S. Tiger milk mushroom (the Lignosus trinity) in Malaysia: a medicinal treasure trove. In: Agrawal DC, Dhanasekaran M, eds. *Medicinal Mushrooms: Recent Progress in Research and Development.* Singapore: Springer Singapore; 2019:349–369.
56. Nallathamby N, Phan CW, Seow SL, et al. A status review of the bioactive activities of tiger milk mushroom Lignosus rhinocerotis (cooke) ryvarden. *Front Pharmacol.* 2017;8:998.
57. Wong XK, Alasalvar C, Ng WJ, Ee KY, Lam MQ, Chang SK. Tiger milk mushroom: a comprehensive review of nutritional composition, phytochemicals, health benefits, and scientific advancements with emphasis on chemometrics and multi-omics. *Food Chem.* 2024;459, 140340.
58. Fernandes A, Rodrigues PM, Pintado M, Tavaria FK. A systematic review of natural products for skin applications: targeting inflammation, wound healing, and photo-aging. *Phytomedicine.* 2023;115, 154824.
59. Arslan NP, Dawar P, Albayrak S, et al. Fungi-derived natural antioxidants. *Crit Rev Food Sci Nutr.* 2023:1–24.
60. Lim HS, Simon SE, Yow YY, Saidur R, Tan KO. Photoprotective activities of Lignosus rhinocerus in UV-irradiated human keratinocytes. *J Ethnopharmacol.* 2022;299, 115621.
61. Fung SY, Yap HY, Ng ST, Tan CS. In vitro inhibition of melanin formation and enhancement of collagen production by a mushroom sclerotial water extract from the tiger milk mushroom, Lignosus rhinocerus (agaricomycetes), with No skin and eye irritation. *Int J Med Mushrooms.* 2022;24(5):19–32.